UDC 54.19

VIBRATIONAL DYNAMICS OF Co$_{67}$Zr$_{33}$ SEMICONDUCTOR GLASSY ALLOY

© 2009   **A.M. Vora***

Parmeshwari 165, Vijaynagar Area, Hospital Road, Bhuj—Kutch, 370 001, Gujarat, India

The computation of vibrational dynamics of semiconductor Co$_{67}$Zr$_{33}$ glassy alloy has been reported for the first time that uses a different theoretical model potential formalism with Wills-Harrison (WH) form. Various local field correction functions are used to study the screening influence. The thermodynamic and elastic properties are also estimated from the elastic limits of the phonon dispersion curves (PDC). The dispersion frequency with respect to the wavenumber is found to be influenced by the dielectric screening due to the conduction electrons. Values obtained using the S-local field correction function and BS approach tend to be greater than other values calculated.

K e y w o r d s: Co, Zr, pair potential, semiconductor glassy alloy, phonon dispersion curves (PDC), thermodynamic properties, elastic properties.

INTRODUCTION

The research on intertransition metals based binary alloys has followed from the desire to understand the mechanisms responsible for their physical and electronic properties. Examples of significant problems include the conditions under which amorphous or crystalline phases form, and the technological origins of negative temperature coefficients of electrical resistance. At a basic level all of these properties must be controlled by the electronic structure of the valence electrons. Theoretical understanding of these structures has been difficult to achieve because of the lack of translational symmetry, both for disordered crystalline alloys and amorphous or glassy alloys. The possible application of transition metal alloys is in microelectronics or as thin-film coating [1].

The composition dependence of viscous flow and atomic motion in undercooled metallic glass forming liquids like Co$_{100-x}$Zr$_x$ has been studied by Rößler and Teichler [2] using MD technique. Hence, the present exploratory study considers the Co$_{100-x}$Zr$_x$ system as a typical example of a transition metallic glass. The binary system was chosen to keep the situation as simple as possible. Very recently we have reported vibrational dynamics of some metallic glasses using model potential formalism [3—11]. The theoretical computations of vibrational dynamics of Co$_{67}$Zr$_{33}$ glassy alloy has been reported for the first time in the present article in terms of the two longitudinal and transverse modes by employing three different approaches *viz.* Hubbard—Beeby (HB) [12], Takeno—Goda (TG) [13, 14] and Bhatia—Singh (BS) [15, 16]. The pair potential has been calculated using the extended theory of Wills—Harrison (WH) [17]. The well recognized model potential Gajjar et al. [3—11] is used with Hartree (H) [18], Taylor (T) [19], Ichimaru—Utsumi (IU) [20], Farid et al. (F) [21] and Sarkar et al. (S) [22] local field correction functions for the first time in the present study. The thermodynamic and elastic properties such as longitudinal sound velocity υ_L, transverse sound velocity υ_T, isothermal bulk modulus B$_T$, modulus of rigidity G, Poisson′s ratio σ, Young′s modulus Y, Debye

---

* E-mail: voraam@yahoo.com

temperature θ_D and low temperature specific heat capacity C_V have been calculated from the elastic limit of the phonon dispersion curves (PDC).

The Vegard's law was used to explain electron-ion interaction for binaries, but it is well known that the pseudo-alloy-atom (PAA) is a more meaningful approach to explain such kind of interactions in binary alloys [3—11]. Hence, in the present article the PAA model is used to investigate the vibrational dynamics of binary $Co_{67}Zr_{33}$ glassy system.

COMPUTATIONAL TECHNIQUE

The fundamental component of the vibrational dynamics of metallic glasses is the pair potential. In the present study, the pair potential is computed using Wills—Harrison (WH) approach [3—11, 17]:

$$V(r) = V_S(r) + \left[-Z_d \left(1 - \frac{Z_d}{10}\right) \left(\frac{12}{N_C}\right)^{1/2} \left(\frac{28.06}{\pi}\right) \frac{2r_d^3}{r^5} \right] + Z_d \left(\frac{450}{\pi^2}\right) \frac{r_d^6}{r^8}. \tag{1}$$

The s-electron contribution to the pair potential $V_S(r)$ is calculated from the expression [3—11]:

$$V_s(r) = \left(\frac{Z_S^2 e^2}{r}\right) + \frac{\Omega_O}{\pi^2} \int F(q) \left[\frac{Sin(qr)}{qr}\right] q^2 \, dq, \tag{2}$$

where Ω_O is the atomic volume of the one component fluid.

The energy wave number characteristics appearing in the Equation (2) is written as [3—11]

$$F(q) = \frac{-\Omega_O q^2}{16\pi} |W_B(q)|^2 \frac{[\varepsilon_H(q)-1]}{\{1 + [\varepsilon_H(q)-1][1-f(q)]\}}. \tag{3}$$

Here $W_B(q)$, $\varepsilon_H(q)$, $f(q)$ are the bare ion potential, the Hartree dielectric response function and the local field correction functions to introduce the exchange and correlation effects, respectively. In the present computation, the $Z_S \sim 1.5$ is taken and parameters Z_d and r_d are obtained from the band structure data [3—11, 17].

The well recognized model potential $W_B(q)$ of Gajjar et al. [3—11] used in the present computation of phonon dynamics of binary metallic glasses is of the form

$$W_B(q) = \frac{-4\pi e^2 Z}{\Omega_O q^2} \left[\begin{array}{l} \left\{ \begin{array}{l} -1 + \dfrac{12}{U^2} + \dfrac{U^2}{1+U^2} + \dfrac{6U^2}{(1+U^2)^2} + \dfrac{18U^2}{(1+U^2)^3} - \dfrac{6U^4}{(1+U^2)^3} \\ + \dfrac{24U^2}{(1+U^2)^4} - \dfrac{24U^4}{(1+U^2)^4} \end{array} \right\} \cos(U) \\ + \\ \left\{ \begin{array}{l} \dfrac{6}{U} - \dfrac{12}{U^3} + \dfrac{U}{1+U^2} + \dfrac{3U}{(1+U^2)^2} - \dfrac{3U^3}{(1+U^2)^2} + \dfrac{6U}{(1+U^2)^3} \\ - \dfrac{18U^3}{(1+U^2)^3} + \dfrac{6U}{(1+U^2)^4} - \dfrac{36U^3}{(1+U^2)^4} + \dfrac{6U^5}{(1+U^2)^4} \end{array} \right\} \sin(U) \\ + \\ \left\{ \begin{array}{l} \dfrac{6}{U} - \dfrac{12}{U^3} + \dfrac{U}{1+U^2} + \dfrac{3U}{(1+U^2)^2} - \dfrac{3U^3}{(1+U^2)^2} + \dfrac{6U}{(1+U^2)^3} \\ - \dfrac{18U^3}{(1+U^2)^3} + \dfrac{6U}{(1+U^2)^4} - \dfrac{36U^3}{(1+U^2)^4} + \dfrac{6U^5}{(1+U^2)^4} \end{array} \right\} \sin(U) \end{array} \right]. \tag{4}$$

Here $U = qr_C$. r_C is the model potential parameter. This form has feature of a Coulombic term outside the core and varying cancellation due to repulsive and attractive contributions to the potential within the core in real space. The detailed information of this potential is given in the literature [3—11].

The model potential parameter r_C is calculated from the well known formula [23] as follows:

$$r_C = \left[\frac{0.51\, r_S}{(Z)^{1/3}}\right], \tag{5}$$

where Z, r_S are the effective valence and effective Wigner—Seitz radius of the component, respectively. The three theories for studying phonons in amorphous alloys proposed by HB [12], TG [13, 14] and BS [15, 16] have been employed for studying the longitudinal and transverse phonon frequencies in binary metallic glass.

According to the HB [12], the expressions for longitudinal and transverse phonon frequencies are:

$$\omega_L^2(q) = \omega_E^2 \left[1 - \frac{\sin(q\sigma)}{q\sigma} - \frac{6\cos(q\sigma)}{(q\sigma)^2} + \frac{6\sin(q\sigma)}{(q\sigma)^3}\right], \tag{6}$$

$$\omega_T^2(q) = \omega_E^2 \left[1 - \frac{3\cos(q\sigma)}{(q\sigma)^2} + \frac{3\sin(q\sigma)}{(q\sigma)^3}\right], \tag{7}$$

where $\omega_E^2 = \left(\frac{4\pi\rho}{3M}\right)\int_0^\infty g(r)V''(r)r^2 dr$ is the maximum frequency.

Following to TG [13, 14], the wave vector (q) dependent longitudinal and transverse phonon frequencies are written as

$$\omega_L^2(q) = \left(\frac{4\pi\rho}{M}\right)\int_0^\infty dr\, g(r)\left[\left\{rV'(r)\left(1 - \frac{\sin(qr)}{qr}\right)\right\} + \right.$$
$$\left. + \{r^2V''(r) - rV'(r)\}\left(\frac{1}{3} - \frac{\sin(qr)}{qr} - \frac{2\cos(qr)}{(qr)^2} + \frac{2\sin(qr)}{(qr)^3}\right)\right], \tag{8}$$

$$\omega_T^2(q) = \left(\frac{4\pi\rho}{M}\right)\int_0^\infty dr\, g(r)\left[\left\{rV'(r)\left(1 - \frac{\sin(qr)}{qr}\right)\right\} + \right.$$
$$\left. + \{r^2V''(r) - rV'(r)\}\left(\frac{1}{3} + \frac{2\cos(qr)}{(qr)^2} + \frac{2\sin(qr)}{(qr)^3}\right)\right]. \tag{9}$$

According to modified BS [15, 16] approach, the phonon frequencies of longitudinal and transverse branches are given by

$$\omega_L^2(q) = \frac{2N_C}{\rho q^2}(\beta I_0 + \delta I_2) + \frac{k_e\, k_{TF}^2\, q^2\, |G(qr_S)|^2}{q^2 + k_{TF}^2\, \varepsilon(q)}, \tag{10}$$

$$\omega_T^2(q) = \frac{2N_C}{\rho q^2}\left(\beta I_0 + \frac{1}{2}\delta(I_0 - I_2)\right). \tag{11}$$

Other details of the constants used in this approach were already narrated in the literature [15, 16]. Here M, ρ are the atomic mass and the number density of the glassy component, while $V'(r)$ and $V''(r)$ are the first and second derivative of the pair potential, respectively.

In the long-wavelength limit of the frequency spectrum, both phonon frequencies, i.e. transverse and longitudinal, are proportional to the wave vector (q) and obey the relationships:

$$\omega_L \propto q \;\; \text{and} \;\; \omega_T \propto q,$$
$$\omega_L = \upsilon_L q \;\; \text{and} \;\; \omega_T \propto \upsilon_T q, \tag{12}$$

where υ_L and υ_T are the longitudinal and transverse sound velocities of the metallic glasses respectively. For the three approaches the equations are:

For HB [12] approach, the formulations for υ_L and υ_T are given by

$$\upsilon_L(\text{HB}) = \omega_E \sqrt{\frac{3\sigma^2}{10}} \tag{13}$$

and

$$\upsilon_T(\text{HB}) = \omega_E \sqrt{\frac{\sigma^2}{10}}. \tag{14}$$

In TG [13, 14] approach, the expressions for υ_L and υ_T are written by

$$\upsilon_L(\text{TG}) = \left[\left(\frac{4\pi\rho}{30\,M} \right) \int_0^\infty dr\, g(r)\, r^3\, \{rV''(r) - 4V'(r)\} \right]^{1/2} \tag{15}$$

and

$$\upsilon_T(\text{TG}) = \left[\left(\frac{4\pi\rho}{30\,M} \right) \int_0^\infty dr\, g(r)\, r^3\, \{3rV''(r) - 4V'(r)\} \right]^{1/2}. \tag{16}$$

The formulations for υ_L and υ_T in BS [15, 16] approach are as follows:

$$\upsilon_L(\text{BS}) = \left[\frac{N_C}{\rho} \left(\frac{1}{3}\beta + \frac{1}{5}\delta \right) + \frac{k_e}{3} \right]^{1/2} \tag{17}$$

and

$$\upsilon_T(\text{BS}) = \left[\frac{N_C}{\rho} \left(\frac{1}{3}\beta + \frac{1}{15}\delta \right) \right]^{1/2}. \tag{18}$$

In the long-wavelength limit of the frequency spectrum, transverse and longitudinal sound veloci-ties υ_L and υ_T are computed. The isothermal bulk modulus B_T, modulus of rigidity G, Poisson′s ratio σ, Young′s modulus Y and the Debye temperature θ_D are found using the expressions [3—11]:

$$B_T = \rho_M \left(\upsilon_L^2 - \frac{4}{3}\upsilon_T^2 \right), \tag{19}$$

$$G = \rho_M\, \upsilon_T^2, \tag{20}$$

where ρ_M is the isotropic number density of the solid;

$$\sigma = \frac{1 - 2\left(\dfrac{\upsilon_T^2}{\upsilon_L^2} \right)}{2 - 2\left(\dfrac{\upsilon_T^2}{\upsilon_L^2} \right)}, \tag{21}$$

$$Y = 2G(\sigma + 1), \tag{22}$$

$$\theta_D = \frac{\hbar\omega_D}{k_B} = \frac{\hbar}{k_B} 2\pi \left[\frac{9\rho}{4\pi} \right]^{1/3} \left[\frac{1}{\upsilon_L^3} + \frac{2}{\upsilon_T^3} \right]^{(-1/3)}, \tag{23}$$

where ω_D is the Debye frequency.

The low temperature specific heat C_V is obtained from Kovalenko and Krasny [24],

$$C_V = \frac{\Omega_O\,\hbar^2}{k_B\,T^2} \sum_{\lambda = L,T} \int \frac{d^3q}{(2\pi)^3} \frac{\omega_\lambda^2(q)}{\left[\exp\left(\dfrac{\hbar\omega_\lambda(q)}{k_B\,T} \right) - 1 \right] \left[1 - \exp\left(-\dfrac{\hbar\omega_\lambda(q)}{k_B\,T} \right) \right]}. \tag{24}$$

The basic feature of temperature dependence of C_V is determined by the behavior of $\omega_\lambda(q)$, where $\hbar$, k_B, T and ω_D are the Plank′s constant, Boltzmann constant, temperature and Debye frequency of the glassy system, respectively.

Fig. 1. Dependence on screening of pair potential for $Co_{67}Zr_{33}$ glassy alloy

RESULTS AND DISCUSSION

The input parameters and other related constants used in the present computations, i.e. $Z = 2.66$, $\Omega_O = 1.5121 \propto 10^{-23}$ cm^3, $N_C = 12.00$, $M = 1.1552 \times 10^{-22}$ gm, $\rho = 7.6407$ gm/cm^3 and $r_C = 4.0752 \times 10^{-9}$ cm, are calculated from the pure metallic data of the semiconductor glassy alloy.

The presently computed pair potentials of $Co_{67}Zr_{33}$ glass are displayed in Fig. 1. It is apparent from the Fig. that the inclusions of exchange and correlation effects do not affect significantly the behavior of the pair potentials. The first zero for $V(r = r_0)$ due to all local field correction functions occurs at $r_0 \approx 5.2$ au. The position of $V_{min}(r)$ is not highly affected by the nature of the screening and the oscillatory nature is also absent at large r-region. The Coulomb repulsive potential part dominates the oscillations due to ion-electron-ion interactions, which show the waving shape of the potential after 10 au. Hence, the pair potentials converge towards a finite value instead of zero in attractive region.

The PCF computed theoretically through the effective interatomic pair potential is shown in Fig. 2. It is found that the peak positions due to S show higher values while those due to H show lower. The screening effect is observed in the nature of the PCF. The ratio (r_2/r_1) of the position of the second peak (r_2) to that of the first peak (r_1) is found to be 1.46, 1.56, 1.51, 1.51 and 1.59 for H, T, IU, F and S, respectively. The ratio (r_3/r_1) of the position of the third peak (r_3) to that of the first peak (r_1), i.e. the ratio of the third atomic shell radius to the nearest-neighbour distance, is found to be 2.00, 2.16, 2.07, 2.07 and 2.18 for H, T, IU, F and S, respectively. All the ratios found are in fair agreement with the reported values of Co in amorphous state, i.e. $(r_2/r_1) = 1.65$, 1.69 and $(r_3/r_1) = 1.93$, 1.93 [25]. The (r_2/r_1) ratio is close to the c/a ratio in close-packed hexagonal structure, i.e. $c/a = 1.63$, which suggests that the short range order of nearest neighbours is influenced more or less by the atomic arrangement of the crystal structure. This result is typical of a metallic glass with a large main peak at the nearest-nearest distance followed by smaller peaks corresponding to more distant neighbours. The main peak is sharp because 'Co' and 'Zr' are comparable in size. Actually, it is very difficult to draw conclusions regarding the disorder visible after 15 Å in Fig. 2, because the experimental data is not available for this glass. Actually, this long range order is normal and it may be due to the waving shape of the pair potential.

The results shown in Fig. 3 are the phonon frequencies generated using HB approach with the five screening functions for studying the screening influence. It is seen that the inclusion of exchange and correlation effect raises the phonon frequencies in both longitudinal as well as transverse branches. The first minimum in the longitudinal branch is around $q \approx 1.9$ Å^{-1} for H, $q \approx 2.6$ Å^{-1} for T, $q \approx 2.5$ Å^{-1} for IU as well as F and $q \approx 2.7$ Å^{-1} for S-local field correction function. The influence of $f(q)$ s on ω_L at first peak due to T-dielectric function is 309.47 %, for IU is 165.85 %, for F is 176.63 % and for S-screening is 695.93 % with respect to H-dielectric function. Such screening variation on ω_T at $q \approx 1.0$ Å^{-1} due to T, IU, F and S-screening is 242.98 %, 128.17 %, 137.40 % and 539.75 %, respectively.

The PDC calculated from the HB, TG and BS approaches with S-local field correction function are shown in Fig. 4. The first minimum in the longitudinal branch falls at $q \approx 2.7$ Å^{-1} for HB, $q \approx 2.7$ Å^{-1} for TG and $q \approx 1.6$ Å^{-1} for BS approach. The first crossing position of ω_L and ω_T in the HB, TG and BS approaches is seen at 2.1 Å^{-1}, 2.0 Å^{-1} and 1.4 Å^{-1}, respectively. Moreover, the present outcome of PDC due to BS approach is higher than those due to HB and TG approaches.
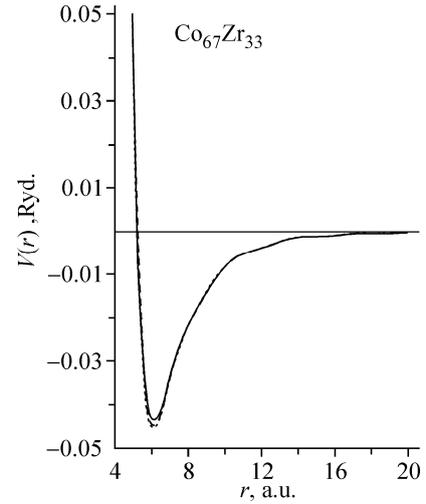
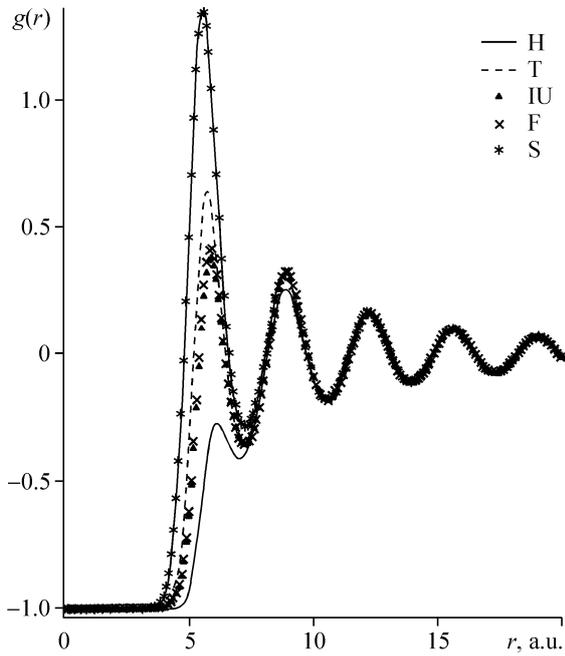*Fig. 2.* Dependence on screening of pair correlation function for $Co_{67}Zr_{33}$ glassy alloy

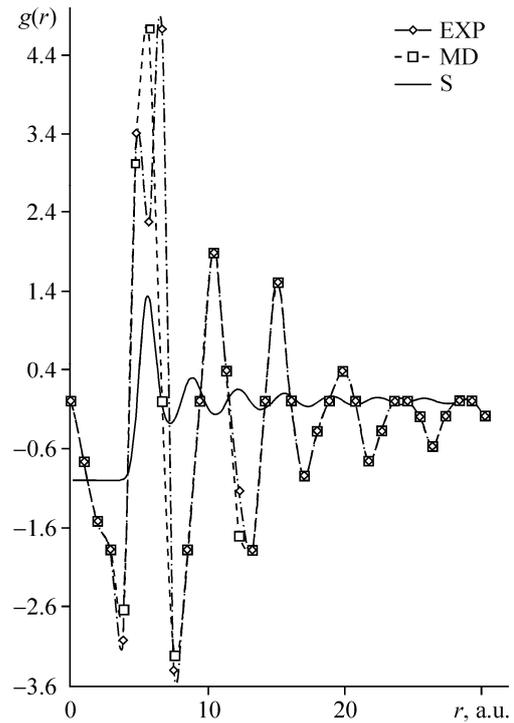*Fig. 3.* Pair correlation function using S-function of $Co_{67}Zr_{33}$ glassy alloy

As shown in Fig. 5, the mode of calculating phonon frequencies affects the anomalous behaviour of the specific heat C_V. In low temperature region high bump is observed in HB and TG approaches, while linear nature is seen in BS approach as it is shown in Fig. 6. The ′anomalous linear′ nature
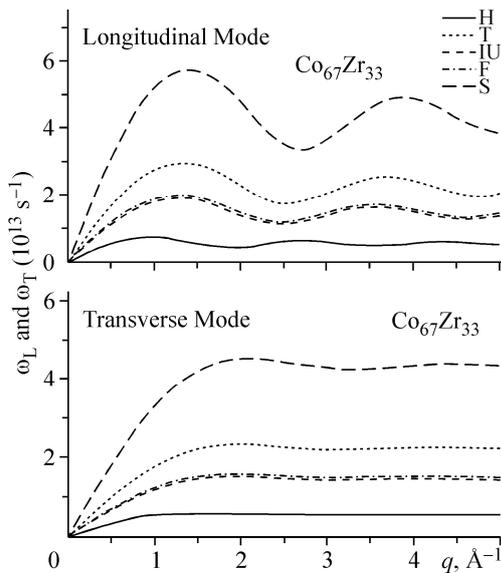

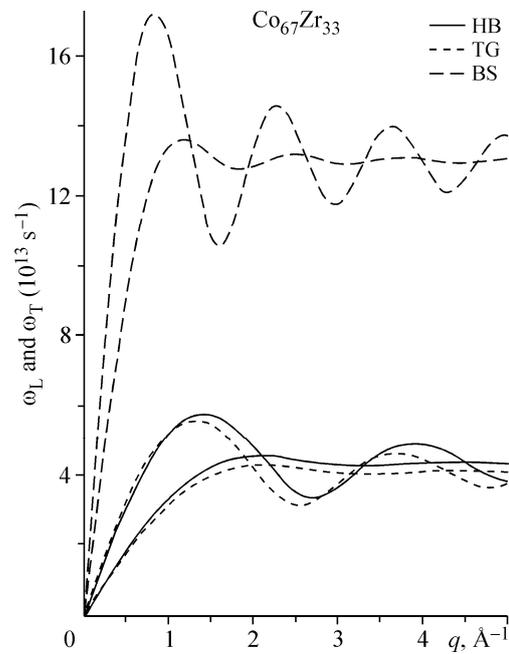*Fig. 4.* Dependence on screening of phonon dispersion curves for $Co_{67}Zr_{33}$ glassy alloy using HB approach

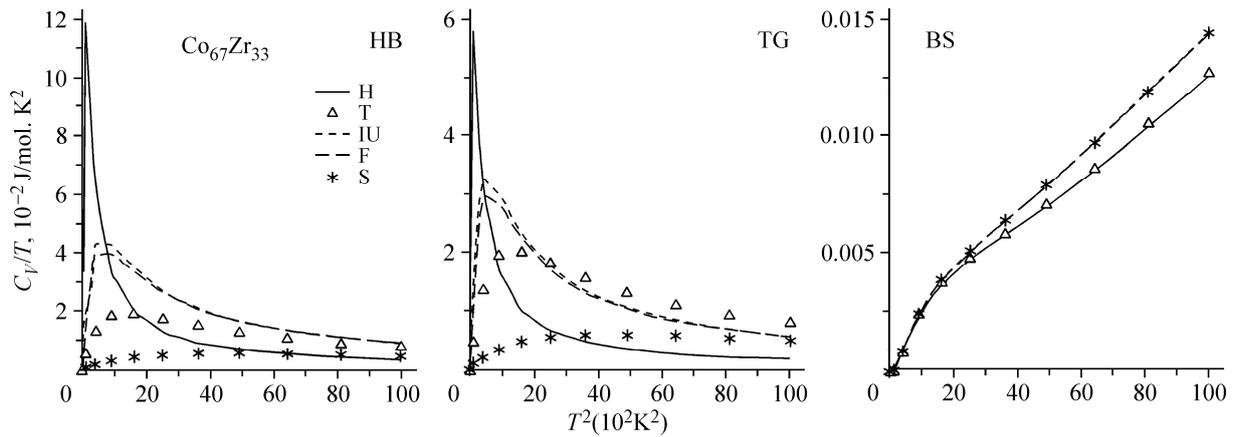*Fig. 5.* Phonon dispersion curves for $Co_{67}Zr_{33}$ glassy alloy using HB, TG and BS approaches with S-functions

Fig. 6. Low temperature specific heat of Co$_{67}$Zr$_{33}$ glassy alloy using HB, TG and BS approaches

appears to be predominant in disordered materials containing low coordinated atoms. The computation of C_V is performed up to the elastic limits of the PDC, i.e. low coordinated atoms only, which produced the ′anomalous linear′ nature. After the elastic limit of the PDC, atoms highly oscillate, that most probably affected the nature of the C_V.

From the elastic limit of the phonon frequency spectrum, the longitudinal and transverse sound velocities have been calculated as reported in Table. The elastic and thermodynamic properties have been calculated using three different approaches given in the same table. Also, one can note from the Table that all the properties calculated using the HB approach give minimum values, while the properties calculated using the BS approach give higher values. The Poisson′s ratio σ remains constant between 0.25—0.30, which shows the elastic behaviour of the system. The obtained yielding is affected by various screening functions used in the present study as well as by the approach adopted for generating PDC.

In all the three approximations, it is very difficult to judge which approximation is the best for computations of vibrational dynamics for Co$_{67}$Zr$_{33}$ glass, because each of his own identity. The HB approach is the simplest and old one; it generates consistent results of the phonon data for this glass

Thermodynamic and Elastic properties of Co$_{67}$Zr$_{33}$ *Glassy Alloy*

Approach	Screening Functions	$\upsilon_L \times 10^5$, cm/s	$\upsilon_T \times 10^5$, cm/s	$B_L \times 10^{11}$, dyne/cm^2	$G \times 10^{11}$, dyne/cm^2	σ	$Y \times 10^{11}$, dyne/cm^2	θ_D, K
HB	H	1.17	0.67	0.58	0.35	0.25	0.87	90.10
	T	3.55	2.05	5.36	3.21	0.25	8.04	274.31
	IU	2.39	1.38	2.42	1.45	0.25	3.64	184.50
	F	2.49	1.44	2.62	1.57	0.25	3.94	191.98
	S	6.52	3.77	18.06	10.84	0.25	27.09	503.65
TG	H	1.88	1.08	1.51	0.88	0.25	2.22	143.97
	T	4.09	2.25	7.62	3.85	0.28	9.89	301.44
	IU	3.05	1.69	4.21	2.18	0.28	5.58	226.81
	F	3.16	1.75	4.50	2.34	0.28	5.98	234.71
	S	6.89	3.70	22.38	10.46	0.30	27.14	497.63
BS	H	19.53	11.94	146.22	108.84	0.20	261.62	1587.56
	T	19.42	11.85	144.90	107.34	0.20	258.25	1576.75
	IU	19.42	11.86	144.84	107.47	0.20	258.47	1577.61
	F	19.43	11.87	145.01	107.62	0.20	258.84	1578.76
	S	19.40	11.84	144.75	107.05	0.20	257.65	1574.71

because the HB approximation needs minimum number of parameters. While TG approach is developed upon the quasi-crystalline approximation where effective force constant depends on the correlation function for the displacement of atoms and correlation function of displacement itself depends on the phonon frequencies. The BS approach retains the interatomic interactions effective between the first nearest neighbours only hence the disorder of the atoms in the formation of metallic glasses is greater showing deviation in magnitude of the PDC as well as in the related properties.

The dielectric function plays an important role in the evaluation of potential due to the screening of the electron gas. For this purpose in the present investigations the local field correction functions due to Hartree (H) [18], Taylor (T) [19], Ichimaru—Utsumi (IU) [20], Farid et al. (F) [21] and Sarkar et al. (S) [22] local field correction functions are used. The reason for selecting these functions is that Hartree (H) [18] function does not include exchange and correlation effect and represents only static dielectric function, while Taylor (T) [19] function covers the overall features of the various local field correction functions proposed before 1972. The Ichimaru—Utsumi (IU) [20], Farid et al. (F) [21] and Sarkar et al. (S) [22] functions are the most recent among the existing functions and they are not exploited rigorously in such studies. This helps us to study the relative effects of exchange and correlation in the aforesaid properties. Hence, the five different local field correction functions show variations up to an order of magnitude in the vibrational properties of the metallic glasses in Figures 3—5.

CONCLUSIONS

Previously, vibrational dynamics has not been investigated theoretically using the IU, F and S-local field correction functions. The PDC generated from the three approaches reproduce all the broad characteristics of dispersion curves. However, the BS approach is found to be more qualitative than the others. The comparison among present results could not be made due to non-availability of theoretical or experimental data. Nevertheless, the present study is very useful as it provides an important set of phonon data for $Co_{67}Zr_{33}$ glass. This study also confirms the applicability of the model potential in the aforesaid properties. Such study on vibrational dynamics of other binary and ternary liquid alloys and metallic glasses is in progress and will be communicated in near future.

REFERENCES

1. *Engelhardt M.A., Jaswal S.S., Sellmyer D.J.* // Phys. Rev. – 1991. – **B44**. – P. 12671.
2. *Rößler U.K., Teichler H.* // Ibid. – 2000. – **E61**. – P. 394.
3. *Gajjar P.N., Vora A.M., Jani A.R.* / In: Proceedings of the 9th Asia Pacific Physics Conference. – Hanoi: The Gioi Publication, Vietnam, 2006.
4. *Vora A.M.* // Chinese Phys. Lett. – 2006. – **23**. – P. 1872.
5. *Vora A.M.* // J. Non-Cryst. Sol. – 2006. – **352**. – P. 3217.
6. *Vora A.M.* // J. Mater. Sci. – 2007. – **42**. – P. 935.
7. *Vora A.M.* // Acta Phys. Pol. – 2007. – **A111**. – P. 859.
8. *Vora A.M.* // Front. Mater. Sci. China. – 2007. – **1**. – P. 366.
9. *Vora A.M.* // Fizika A. – 2008. – **16**. – P. 187.
10. *Vora A.M.* // Romanian J. Phys. – 2008. – **53**. – P. 517.
11. *Vora A.M., Patel M.H., Gajjar P.N., Jani A.R.* // Solid State Phys. India. 2003. – **46**. – P. 315.
12. *Hubbard J., Beeby J.L.* // J. Phys. C: Solid State Phys. – 1969. – **2**. – P. 556.
13. *Takeno S., Goda M.* // Prog. Theor. Phys. – 1971. – **45**. – P. 331.
14. *Takeno S., Goda M.* // Ibid. – 1972. – **47**. – P. 790.
15. *Bhatia A.B., Singh R.N.* // Phys. Rev. – 1985. – **B31**. – P. 4751.
16. *Shukla M.M., Campanha J.R.* // Acta Phys. Pol. – 1998. – **A94**. – P. 655.
17. *Wills J.M., Harrison W.A.* // Phys. Rev. – 1983. – **B28**. – P. 4263.
18. *Harrison W.A.* / in Elementary Electronic Structure. – World Scientific, Singapore, 1999.
19. *Taylor R.* // J. Phys. F: Met. Phys. – 1978. – **8**. – P. 1699.
20. *Ichimaru S., Utsumi K.* // Phys. Rev. – 1981. – **B24**. – P. 7385.
21. *Farid B., Heine V., Engel G., Robertson I.J.* // Ibid. – 1993. – **B48**. – P. 11602.
22. *Sarkar A., Sen D.S., Haldar S., Roy D.* // Mod. Phys. Lett. – 1998. – **B12**. – P. 639.
23. *Hafner J., Heine V.* // J. Phys. F: Met. Phys. – 1983. – **13**. – P. 2479.
24. *Kovalenko N.P., Krasny Y.P.* // Physica B: Condensed Matter. – 1990. – **162**. – P. 115.
25. *Waseda Y.* The Structure of Non-Crystalline Materials. McGraw-Hill Int. Book Com., New York, 1980.